We are IntechOpen,
the world's leading publisher of
Open Access books
Built by scientists, for scientists

4,800
Open access books available

122,000
International authors and editors

135M
Downloads

Our authors are among the

154
Countries delivered to

TOP 1%
most cited scientists

12.2%
Contributors from top 500 universities

BOOK CITATION INDEX

CLARIVATE ANALYTICS
INDEXED

WEB OF SCIENCE™

Selection of our books indexed in the Book Citation Index
in Web of Science™ Core Collection (BKCI)

Interested in publishing with us?
Contact book.department@intechopen.com

Numbers displayed above are based on latest data collected.
For more information visit www.intechopen.com

Preparation of Functionalized Graphene and Gold Nanocomposites – Self-assembly and Catalytic Properties

Jingxin Zhou, Tifeng Jiao, Qingrui Zhang and Jie Hu

Additional information is available at the end of the chapter

http://dx.doi.org/10.5772/62166

Abstract

Nanocomposites and nanomaterials have been attracting more attention in various fields. Nanocomposites can be prepared with a variety of special physical, thermal, and other unique properties. They have better properties than conventional microscale composites and can be synthesized using simple and inexpensive techniques. A composite material consists of an assemblage of two materials of different natures completing and allowing us to obtain a material of which the set of performance characteristics is greater than that of the components taken separately. In our recent research, some functionalized nanocomposites and nanomaterials have been prepared and investigated. In addition, some of the analytical methods, theoretical treatments, and synthetic tools, which are being applied in the area of self-assembly and supramolecular chemistry, will be highlighted. In this chapter, we summarize our main research contributions in recent years in two sections: (1) preparation and catalytic properties of some functionalized graphene nanocomposites; (2) preparation and catalytic properties of some functionalized gold nanocomposites. These works not only provided important inspirations for developing graphene-hybridized materials but also opened new possibilities to improve the photocatalytic activity of photocatalyst.

Keywords: nanocomposites, nanomaterials, catalytic property, self-assembly

1. Introduction

Nanocomposites and nanomaterials have been attracting increasing attention in various fields [1–6]. Nanocomposites can be prepared with a variety of special physical, thermal, and other unique properties. They have better properties than conventional microscale composites and can be synthesized using simple and inexpensive techniques. In addition, as the assemblage

of various separate components, the designed composite materials would demonstrate greater characteristics and performances. At the same time, nanomaterials and nanocomposites often have unique properties that could enable composite materials with multiple unique properties simultaneously; however, it is often challenging to achieve these properties in large-scale nanocomposites and functionalized nanomaterials. In order to obtain the stated objective composites, it is important to design different models of the interactions in nanocomposites and next controllable properties. Moreover, it is well known that various self-assembly techniques are important to fabricate well-defined hierarchical and organized nanostructures with special properties and controlled capacity [7–10]. For different research systems, such as inorganic–organic hybrids, various nanoparticles, colloidal microspheres, and supramolecular nanostructures, the self-assembly process can demonstrate obvious advantages, especially in preparing special nanostructures. The incorporation of nanocomposites with self-assembly shows new performances for designed composite nanomaterial with different organized style and processing routes.

In addition, as a special sp^2-bonded single layer carbon material, graphene has been attracting more attentions in various application fields, especially as photocatalytic material due to its natural characteristics, such as high chemical stability, large surface area, and excellent adsorption capacity [11]. And some new nanocomposites from graphene materials as photocatalysts have been developed in recent years. For example, the research group of Ullah prepared ternary Pt-graphene/TiO_2 nanocomposites by microwave-assisted method and investigated the photocatalytic degradation for dye rhodamine B [12]. Bai and coworkers reported the preparation of new $ZnWO_4$/graphene hybrid materials by in situ reduction of graphene oxide and characterized the degradation capacity of methylene blue as photocatalysts [13]. Sun's group reported the synthesis of $ZnFe_2O_4$/ZnO nanocomposites anchored on graphene substrates via an ultrasound-aided method [14]. Xu and coworkers prepared reduced graphene oxide/Bi_2WO_6 composite materials as photocatalysts, and compared the photocatalytic activities of composites with pure Bi_2WO_6 [15]. In addition, more research works have been reported to enhance the photocatalytic activity of graphene-based composites as photocatalysts [16–19]. Moreover, in the last several decades, the preparations of gold nanoparticles have been attracting much attention [20–22]. Up to now, various processes [23–25] and designed capping agents [26–29] have demonstrated the synthesis of functional gold nanoparticles with designed nanostructures and tailored behaviors. It is well known that many factors, such as the particle size, shape, colloid stability, and surface functionalized groups, seem to be critical for the applications fields [30–32]. In addition, because the self-assembled nanostructures are important and closely related to molecular skeletons in designed template compounds, the design and synthetic routes are the key step in the whole process.

In recent research work reported by our group, various research systems about graphene and gold nanocomposites/nanomaterials have been designed and characterized. And the involved analytical methods and self-assembly techniques have been also highlighted. So in the present chapter, we would like to demonstrate our recent research contributions in two parts: (1) preparation and catalytic properties of some functionalized graphene nanocomposites; (2) preparation and catalytic properties of some functionalized gold nanocomposites. These

works not only provided important inspirations for developing graphene-hybridized materials but also opened new possibilities to improve the photocatalytic activity of photocatalyst.

2. Preparation and catalytic properties of some functionalized graphene nanocomposites

Recently, our group has reported the design and fabrication of hybrid organogels by self-assembly of composites containing cationic compounds and GO [33]. It is interesting to note that the obtained gelation performances can be regulated via different functional substituted headgroups in used compounds. The experimental data indicated that ammonium headgroup in molecular skeletons seemed more favorable for the composite gelation than pyridinium segment. The obtained results suggested that the self-assembly modes in present GO-based composites could be manipulated by controlling efficient headgroup effect. In addition, various weak forces between present building blocks seemed also responsible for the formation of different nanostructures. Based on the obtained results data in present composite gel system, a reasonable mechanism about self-assembly modes in gels is shown in Figure 1. For the prepared CTAB-GO gel, various organized building blocks are obtained in different solvents because of the van der Waals force of substituent chains and the strong electrostatic interaction of ammonium headgroups with oxygen-containing functional groups at GO surface. In addition, for the cases of C16Py-GO and BPy-GO composite gels, the strong π–π stacking between carbon net in GO plane and additional pyridine headgroups showed as more competitive with other forces, such as electrostatic interaction and van der Waals force. Thus, the present research work demonstrates new exploration for the design of GO-based composite gels and self-assembled soft matters.

In addition, we have also demonstrated the formation of organogels by self-assembly of cationic gemini amphiphile–GO composites [34]. Their gelation behaviors in various organic solvents can be controlled by regulating molecular symmetry. The obtained data indicated that the designed functional groups and molecular symmetry could change the self-assembly modes and produce different self-assembled nanostructures. It seemed that longer alkyl chains in molecular skeletons could be helpful to enhance the intermolecular hydrophobic force in the process of self-assembly. So the changes of building blocks and stacking modes between present GO-based composites and different solvents are responsible for the formation of various nanostructures, as seen in Figure 2. It clearly indicated that the formed nanostructures in present composite materials were obviously different, such as nano-wrinkle, nano-lamella, and nano-belt. The obtained different morphologies in self-assembled gels can be mainly due to various formation mechanisms upon special self-assembly modes via weak interactive forces between building blocks. Finally, a reasonable self-assembled mechanism for symmetry effects in formation of present organized nanostructures is demonstrated. Thus, the present GO-based composite gel materials will give a helpful clue for the design and preparation of functional GO composite nanomaterials.
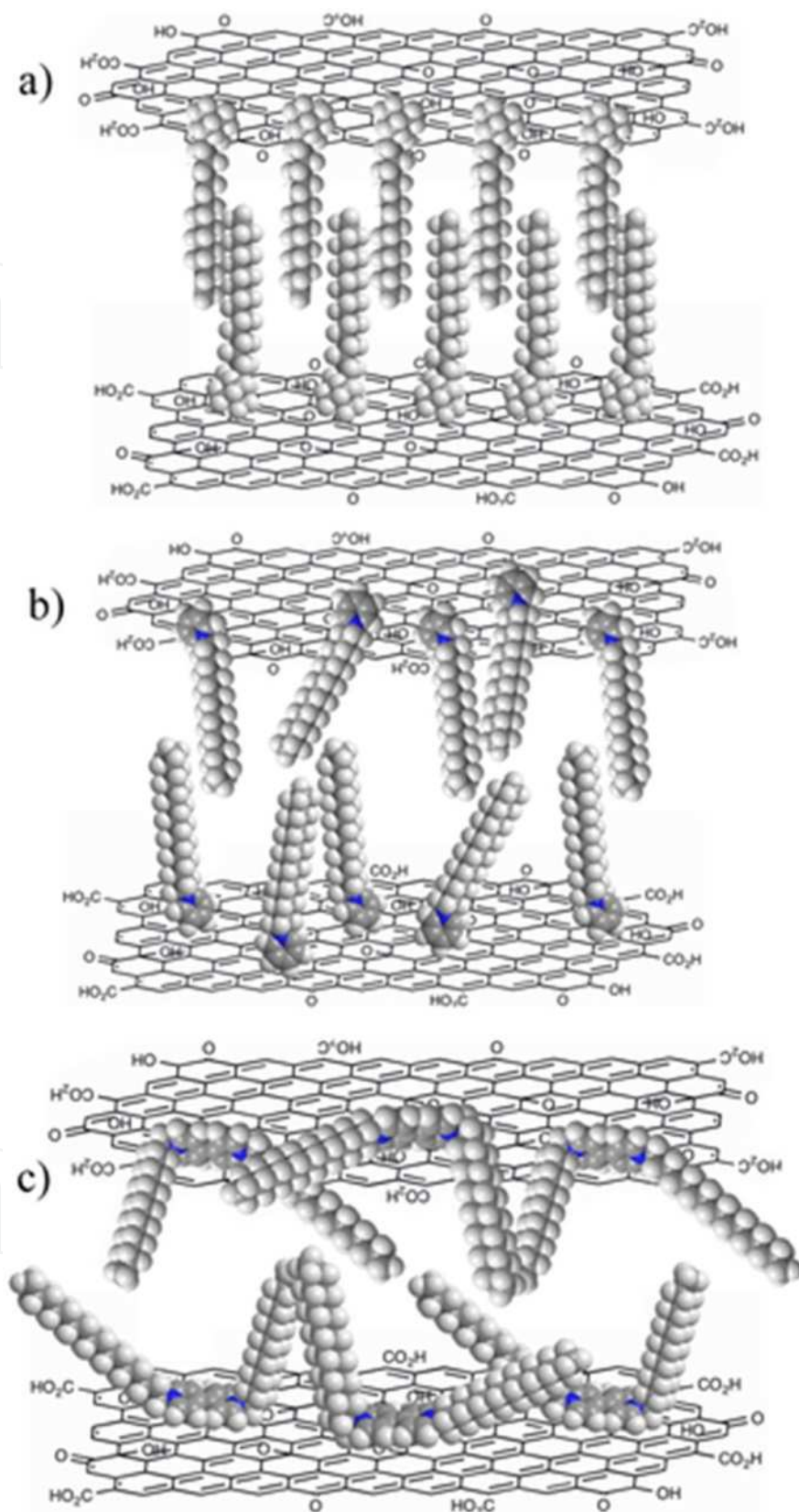
Figure 1. Scheme of different assembly modes in cationic amphiphiles–graphene oxide gels. CTAB-GO (a), C16Py-GO (b), and BPy-GO (c).
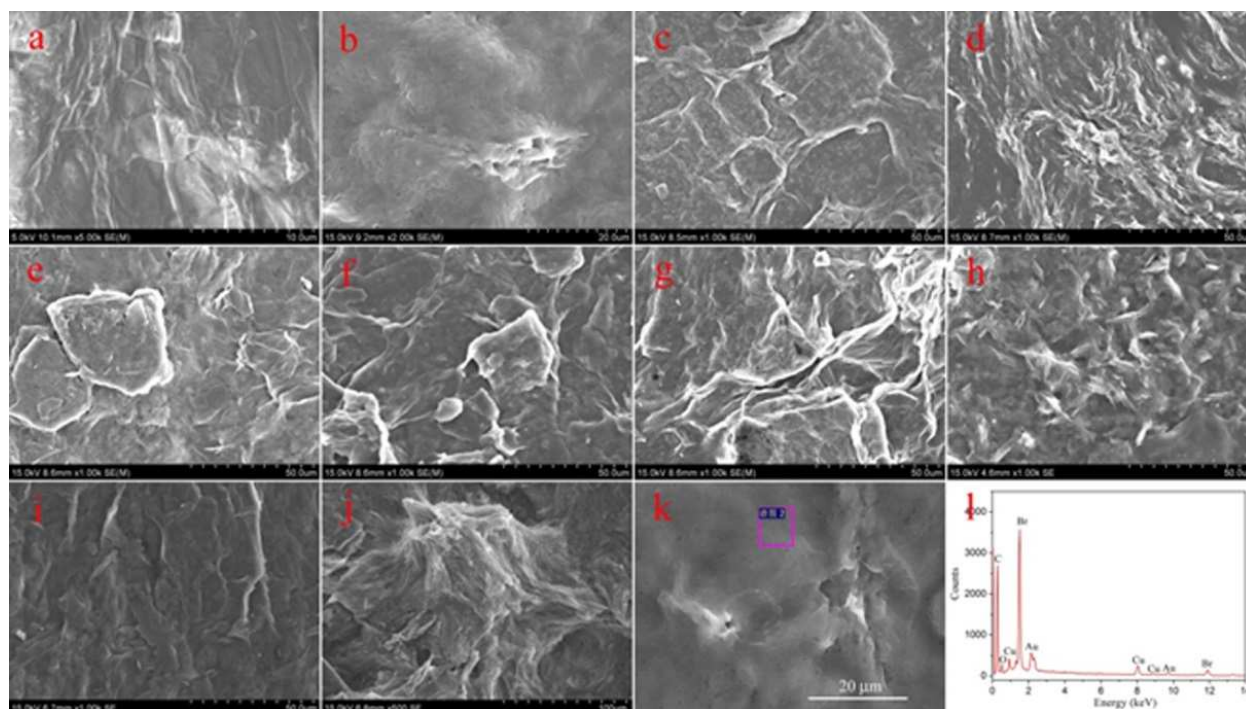
Figure 2. SEM images of xerogels for GO sheet, C18-6-6/GO gels, C18-6-12/GO gels, and C18-6-18/GO gels in different solvents.
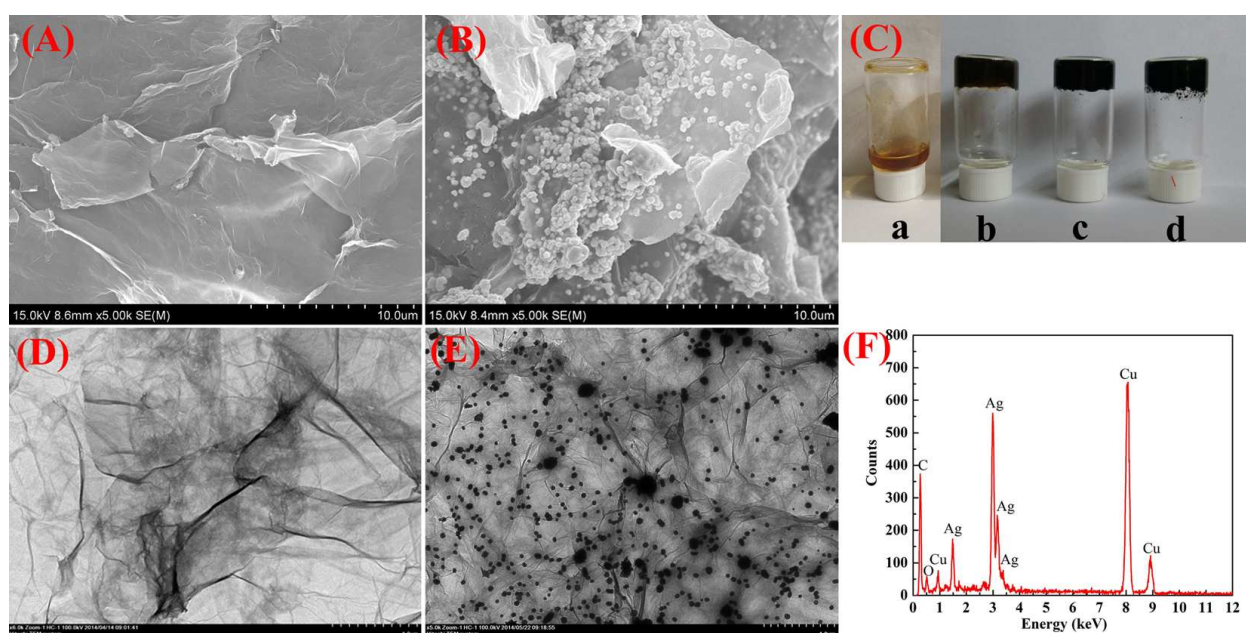

Figure 3. SEM and TEM images for the RGO/PEI and RGO/PEI/Ag hydrogels.

In another composite system, we have reported the design and preparation of silver nanoparticle-containing RGO-based composite hydrogel materials via an in situ reduction process [35]. The obtained experimental data indicated that the prepared composite gels were composed of 3D net-like nanostructures, as seen in Figure 3. In addition, the used preparation method

included the in situ reduction of GO and silver acetate in hydrogel structures to fabricate present RGO-based composite hydrogel. So the formed silver nanoparticles were uniformly anchored on RGO surface in composite gel. Moreover, the photocatalytic behaviors for removing dye pollutants are also characterized for the silver nanoparticle-containing RGO-based composite hydrogel, as seen in Figure 4. It is interesting to note that the obtained photocatalytic composite materials can be reused from an aqueous degradation system, indicating the important and potential applications for dye removal and wastewater treatment.
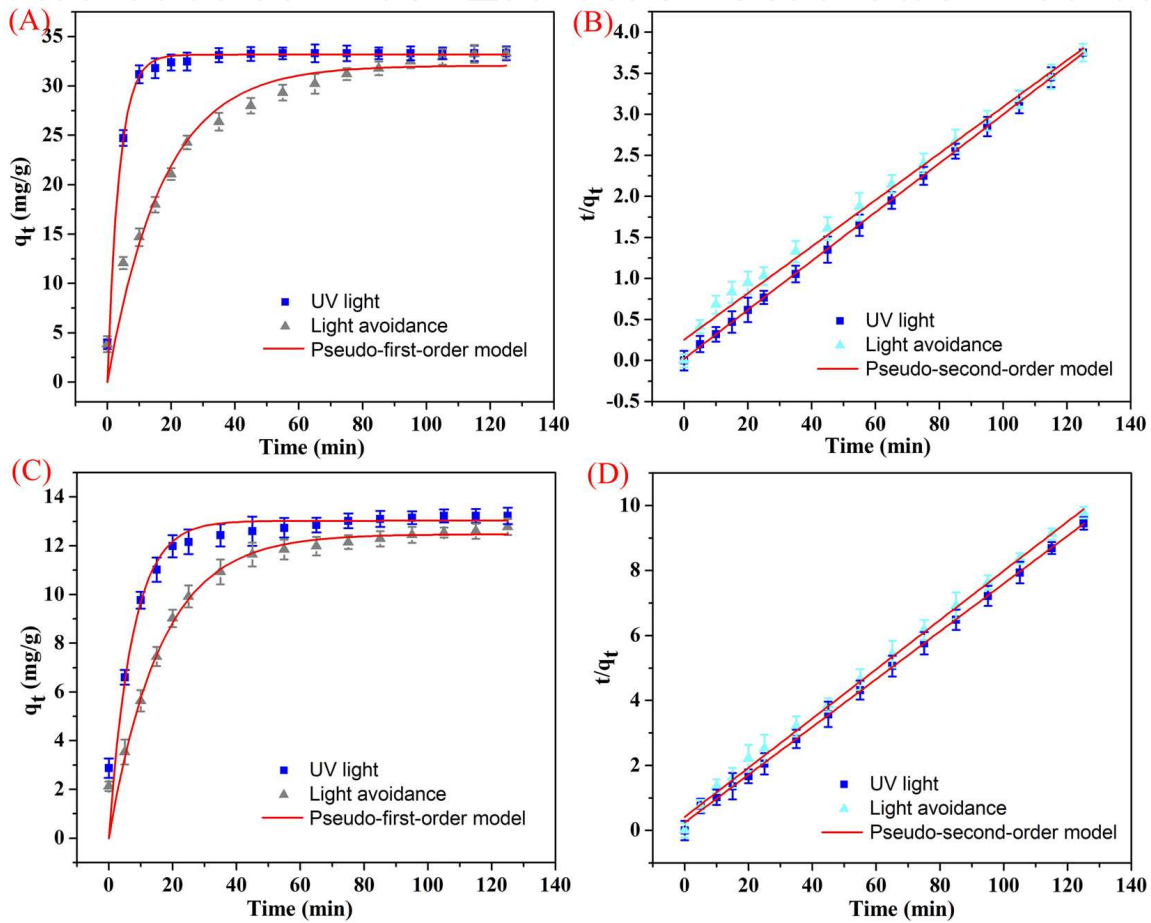

Figure 4. Degradation kinetics curves of as-prepared RGO/PEI/Ag nanocomposites on MB (a, b) and RhB (c, d) at 298 K.

In order to investigate the mechanism of hybrid graphene composites, we have also synthesized some $LaMnO_3$–graphene composites as photocatalysts by a sol–gel method [36]. It is found that $LaMnO_3$ perovskite phase was successfully fixed on graphene surface with well-dispersion capacity, as seen in Figure 5. The data indicated that the photocatalytic capacity of as-formed $LaMnO_3$–graphene composite materials were better than pristine $LaMnO_3$ material, with the detailed results in Figure 6. The enhancement of photocatalytic properties can be mainly due to the high separation efficiency of photo-induced electron–hole pairs originated from the excellent conductivity of graphene in composite and the large interfacial contact between components, which is helpful to increase the dyes adsorption and improve the

transfer efficiency in photocatalytic process. This research demonstrated new inspiration for designing photocatalytic graphene-based hybrid materials.

In another work, organized $La_{1-x}Sr_xMnO_3$/graphene thin films were prepared by both sol–gel and spin-coating methods [37]. In experimental process, the formed sol nanoparticles were adsorbed on graphene surface via electrostatic force in aging time. Then, the formed $LaMnO_3$ nanoparticles increase sizes and form crystal domains on graphene surface in the next calcination step. Present obtained nanostructures and morphology were investigated during various characterization techniques. Figure 7 shows the XRD patterns of graphene, $LaMnO_3$, $LaMnO_3$/graphene, and $La_{0.9}Sr_{0.1}MnO_3$/graphene thin film. The diffraction peak of graphene appeared in the vicinity of 23°, which was similar to the diffraction peak position of graphite. However, this peak broadened and weakened because the size of the graphite sheet decreased, the integrity of the crystal structure declined, and the degree of disorder increased. The pattern of $LaMnO_3$ is in agreement with PDF33-0713, indicating its perovskite structure with complete crystal shape. In the process of acid red 3GN photodegradation, $LaMnO_3$/graphene thin film had sound stability and better photocatalytic ability than $LaMnO_3$ thin film. As shown in Figure 8, a mild photodecomposition effect was observed in the degradation of dye. The absorption peak of acid red 3GN dye solution at 509 nm was from the initial 0.5446 to 0.5138 after irradiating for 48 h without photocatalysts. The experimental results indicated that graphene enhanced the dye adsorption, inhibiting the reunion of light-induced e^-–h^+ and improving photocatalytic capacity. In addition, it should be noted that a red shift of absorption edge was found by doping Sr, which seemed helpful to increase the photocatalytic performance of the obtained composite film.

In addition, another new $LaMn_{1-x}Co_xO_3$/graphene composite material as photocatalyst had been designed and prepared by sol–gel method [38]. The experimental data indicated that $LaMnO_3$ perovskite phase was anchored on graphene surface with the special perovskite structure. In addition, the photocatalytic capacity was characterized by the degradation of diamine green B. In the photodegradation process, the graphene component in composite can accelerate the dye adsorption, while doping Co component improves the photocatalytic performance. Thus, the reasonable charge transfer mechanism that occurred in the obtained $LaMnO_3$/graphene composite during photocatalytic process is demonstrated in Figure 9. Firstly, diamine green B molecules could shift to the active surface of prepared composites from solution and organized in self-assembled face-to-face mode via π–π stacking with aromatic graphene net. Due to the effect of these holes and electron transfers, charge recombination is pushed in obtained $LaMnO_3$/graphene composite and improves the efficiency of photocatalytic capacity.

Moreover, we have also reported the preparation of some graphene-based $LaNiO_3$ composite films by both sol–gel method and spin-coating technique [39]. The obtained experimental results indicated that the size of formed $LaNiO_3$ nanoparticles was about 20 nm, well dispersed on graphene surface. The photocatalytic capacity of present hybrid films had been demonstrated by degradation of acid red A. In comparison with pure $LaNiO_3$ films, the designed $LaNiO_3$/graphene composite films showed better photocatalytic behavior. It is interesting to
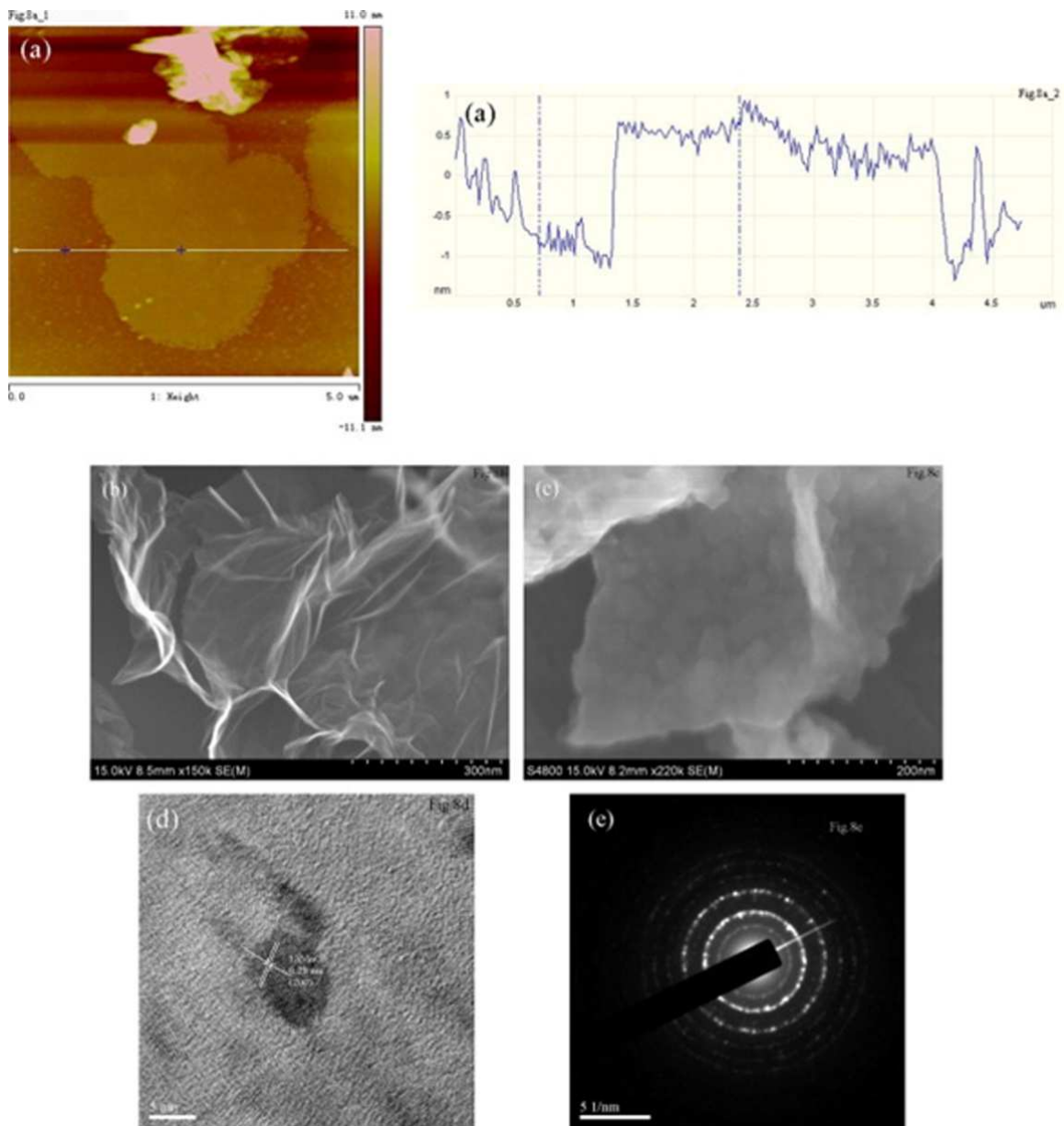
Figure 5. (a) AFM image of the as-synthesized graphene; (b) SEM image of graphene; (c, d, e) SEM, HRTEM, and SA-ED images of LaMnO₃–graphene composites.

note that when the content of graphene shifted to the value of about 4%, the photocatalytic efficiency of the obtained composite films was double that of pure $LaNiO_3$ films.

In another system, $La_{1-x}Ca_xMnO_3$ perovskite–graphene composites are synthesized as catalysts for Zn–air cell cathodes [40]. The results indicated that perovskite phase adhered on the surface of graphene sheets, and adding graphene significantly improved the electrochemical performance of $LaMnO_3$. The XPS spectrum of $La_{0.6}Ca_{0.4}MnO_3$–graphene composite is shown in Figure 10. The peak contained all the elements of $La_{0.6}Ca_{0.4}MnO_3$. In addition, the obtained graphene showed gauze-like fold nanostructures, mainly originated from the oxygenic functional groups and the surface defects during preparation process. So the formed porous
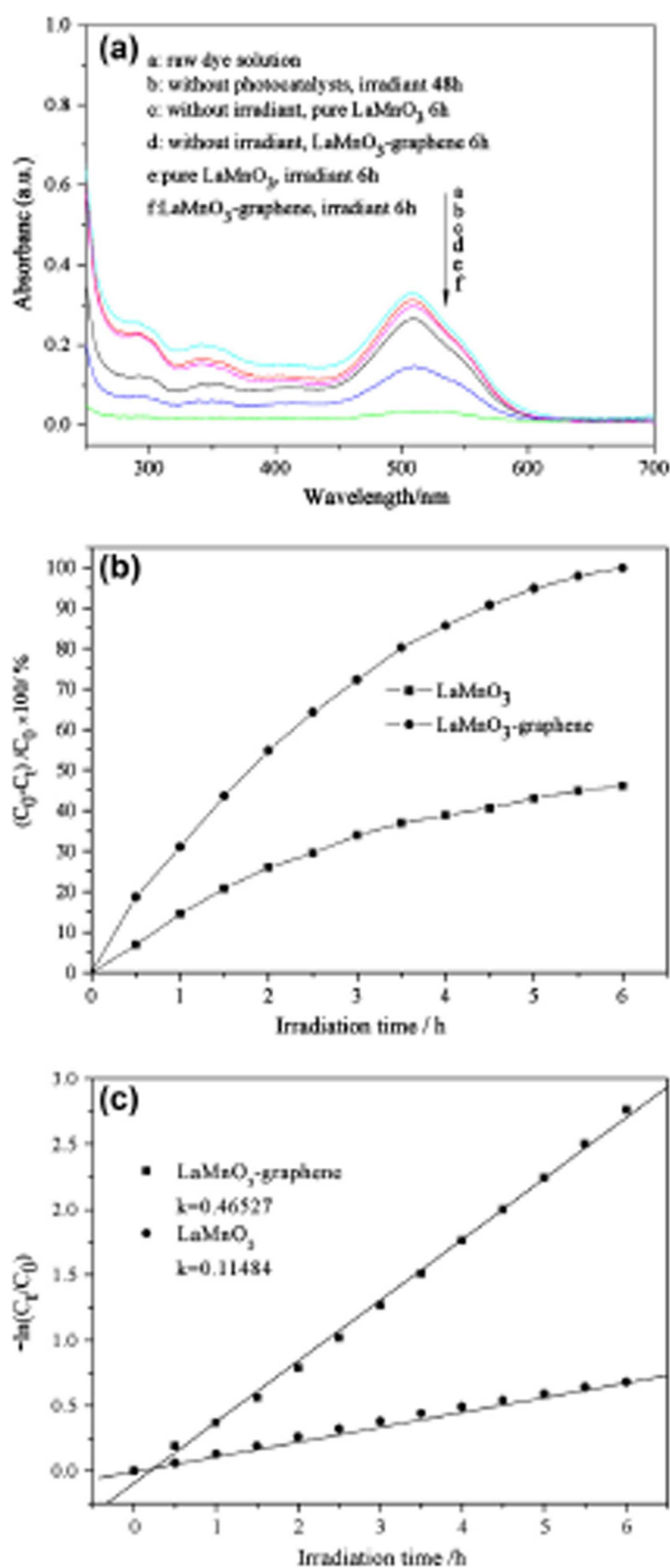
Figure 6. (a) UV–Vis spectral changes of the degradation of acid red A by LaMnO$_3$–graphene and LaMnO$_3$; (b) photocatalytic activities of LaMnO$_3$–graphene composite and LaMnO$_3$; (c) kinetics of photocatalytic degradation by the LaMnO$_3$ and LaMnO$_3$–graphene.
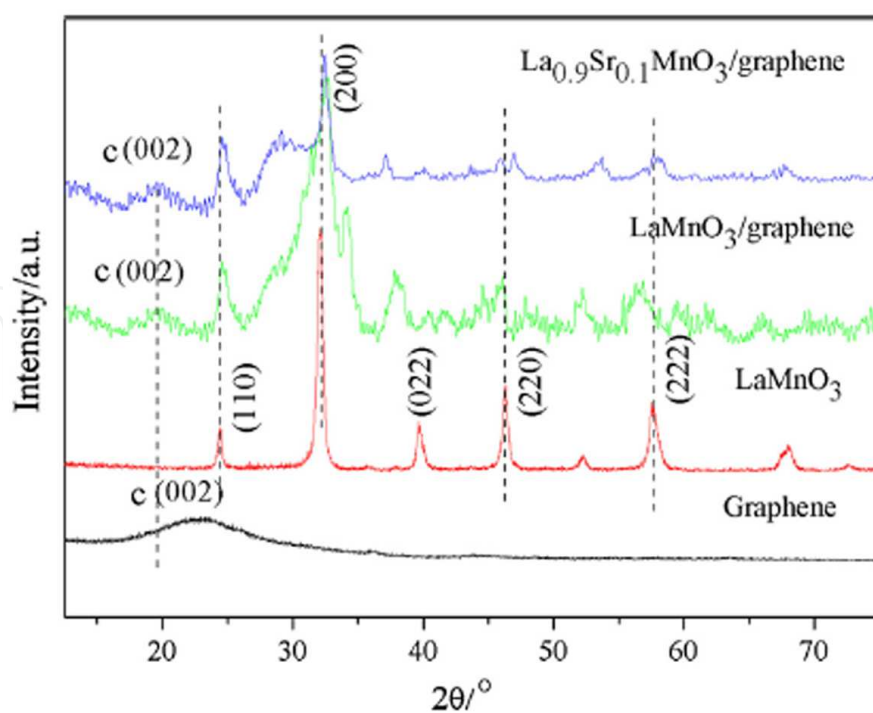
Figure 7. XRD pattern of graphene, LaMnO$_3$, LaMnO$_3$/graphene, and La$_{0.9}$Sr$_{0.1}$MnO$_3$/graphene.
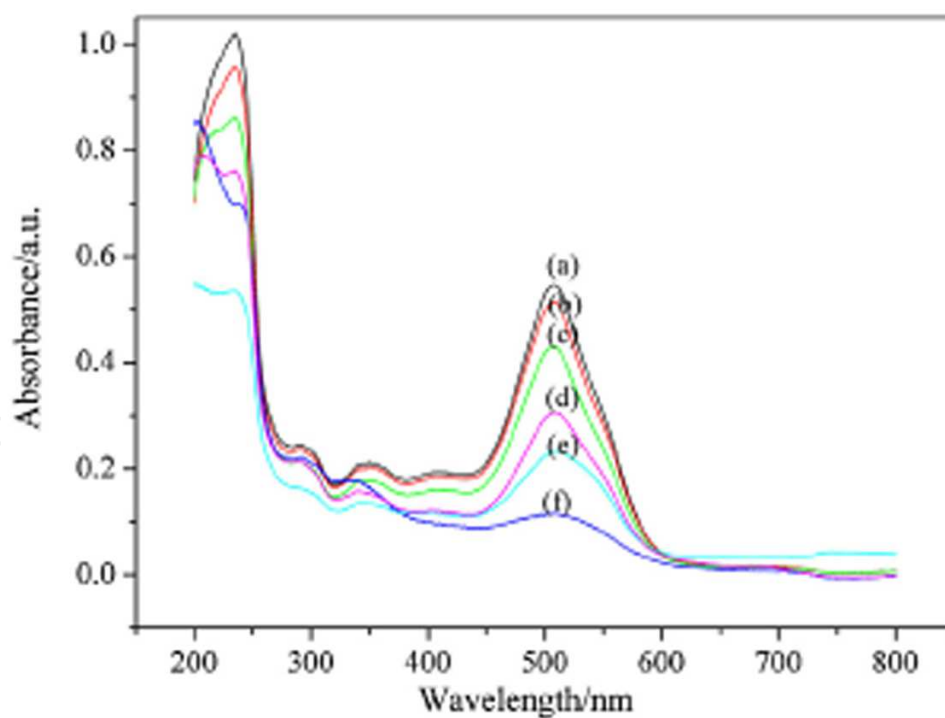
Figure 8. UV–Vis absorb spectrums of acid red-3GN under different conditions: (a) raw dye solution, (b) irradiation 48 h without catalyst, (c) LaMnO$_3$ thin film adsorb dye 4 h without irradiation, (d) LaMnO$_3$/graphene or La$_{0.9}$Sr$_{0.1}$MnO$_3$/graphene thin film adsorb dye 4 h without irradiation, (e) irradiation 4 h with LaMnO$_3$ thin film as catalyst, (f) irradiation 4 h with LaMnO$_3$/graphene thin film as catalyst.
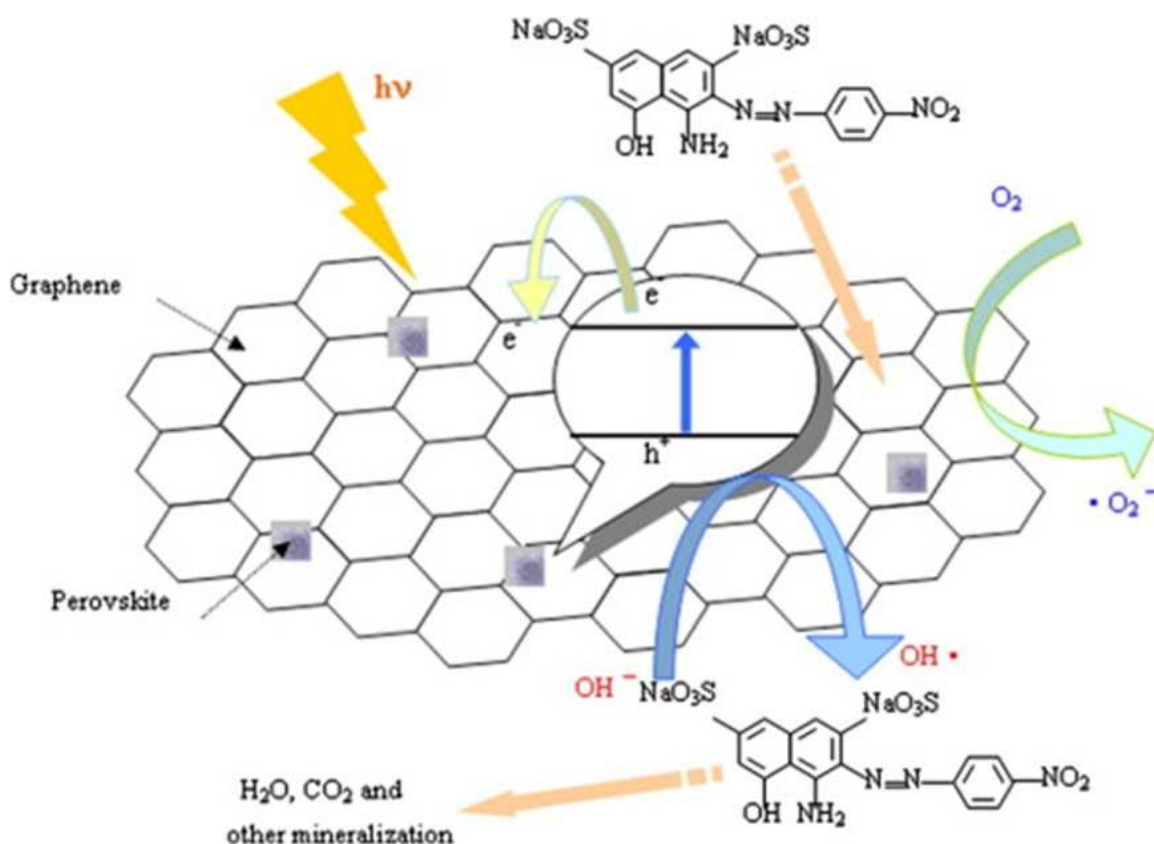
Figure 9. Proposed mechanism for photocatalytic degradation of diamine green B over graphene-based perovskite photocatalysts under light irradiation.

3D nanostructure can obviously enhance the three-phase domains and improve the mass transfer process as catalyst materials of air electrode. The experimental data indicated that the voltage plateau was superior with 10 wt% ratio value of graphene. Moreover, Ca doping maintained the perovskite structure and obviously enhanced the electrocatalytic activity for ORR, and $La_{0.6}Ca_{0.4}MnO_3$–graphene composite demonstrated the best catalytic capacity. Thus, the obtained research work indicates that the prepared graphene-based $La_{1-x}Ca_xMnO_3$ composites are important material for design of air electrodes catalysts.

Recently, we have also reported the preparation of $LaMnO_3$/graphene thin films with the perovskite-type as new photocatalyst via sol–gel process and spin-coating method [41]. The obtained results indicated that the addition of graphene did not change the perovskite structure, with formed $LaMnO_3$ particles at about 22 nm well dispersed on graphene surface. Figure 11 displays the nitrogen adsorption–desorption isotherms and pore size distribution curves calculated by BJH method for $LaMnO_3$ and $LaMnO_3$/graphene powders. The larger surface area can effectively absorb the dye, thus increasing the contact probability of pollutant molecular and catalyst. Determination of contact angle indicated that the contact angle of glass substrate decreased and the hydrophilicity improved after treating with H_2SO_4 and APTES. The UV–Vis photocatalytic activity of the photocatalysts was evaluated by the degradation of diamine green B. $LaMnO_3$/graphene thin films had better photocatalytic ability than $LaMnO_3$ and TiO_2 films.
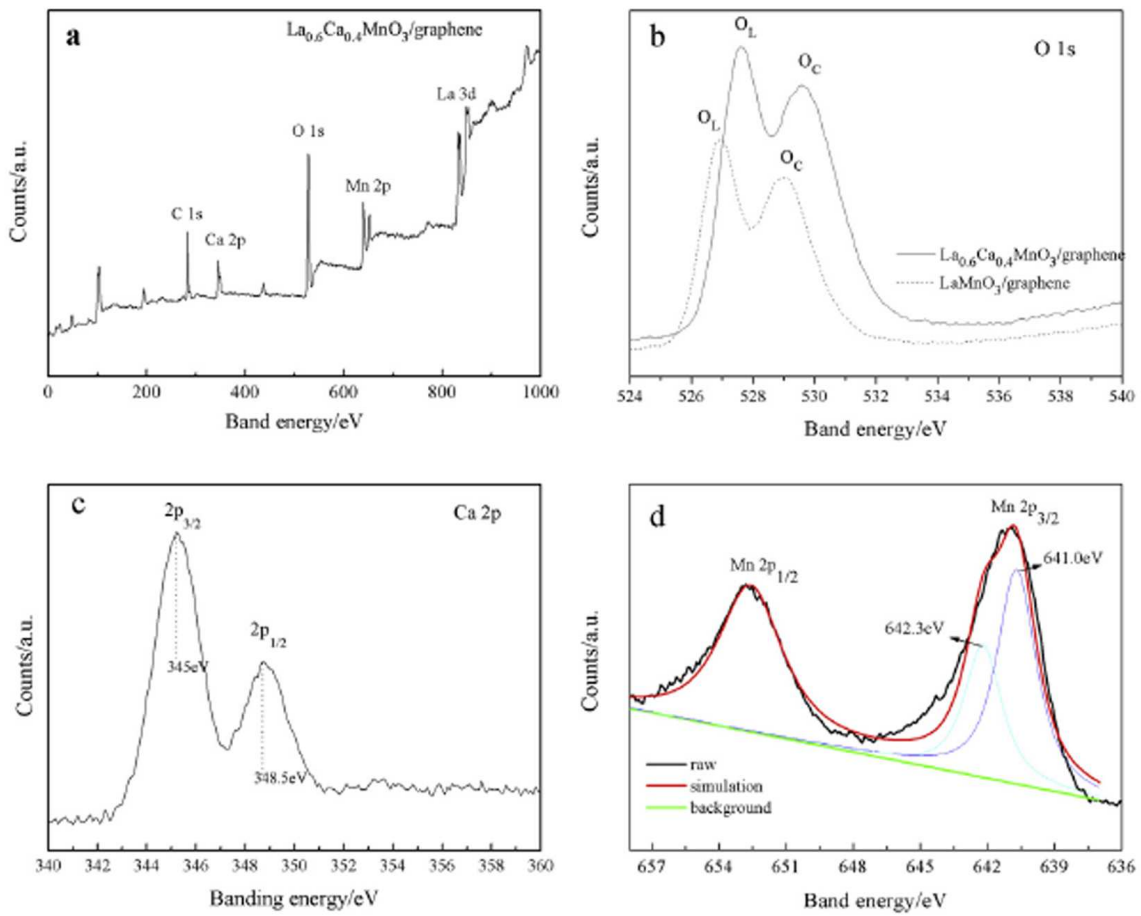
Figure 10. XPS spectrum of $La_{0.6}Ca_{0.4}MnO_3$–graphene composite. (a) Overall spectrum, high-resolution curves of (b) O 1s region, (c) Ca 2p region, and (d) Mn 2p region.
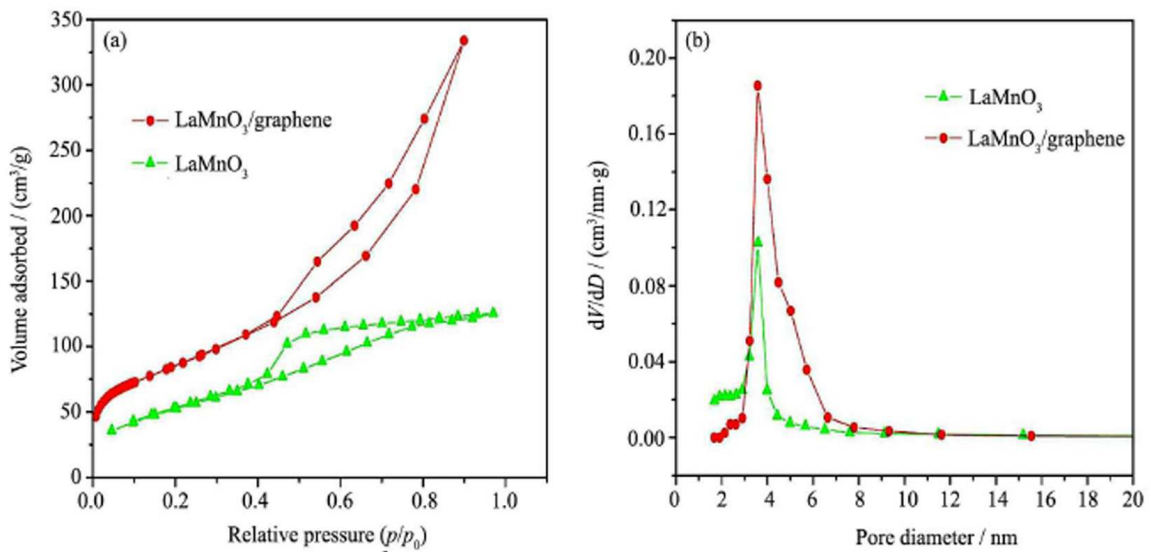

Figure 11. N_2 adsorption–desorption isotherms (a) and pore size distributions of samples (b).

3. Preparation and catalytic properties of some functionalized gold nanocomposites

In this section, many examples have been investigated, including the synthesis of gold nanoparticles by some compounds with hydrophilic spacers and aromatic headgroups at different interface. The obtained experimental data indicated that various gold nanostructures could be prepared by controlling different substituted headgroups in template compounds. In addition, the photocatalytic capacities of as-prepared gold nanoparticles on the degradation of organic dyes were also demonstrated.
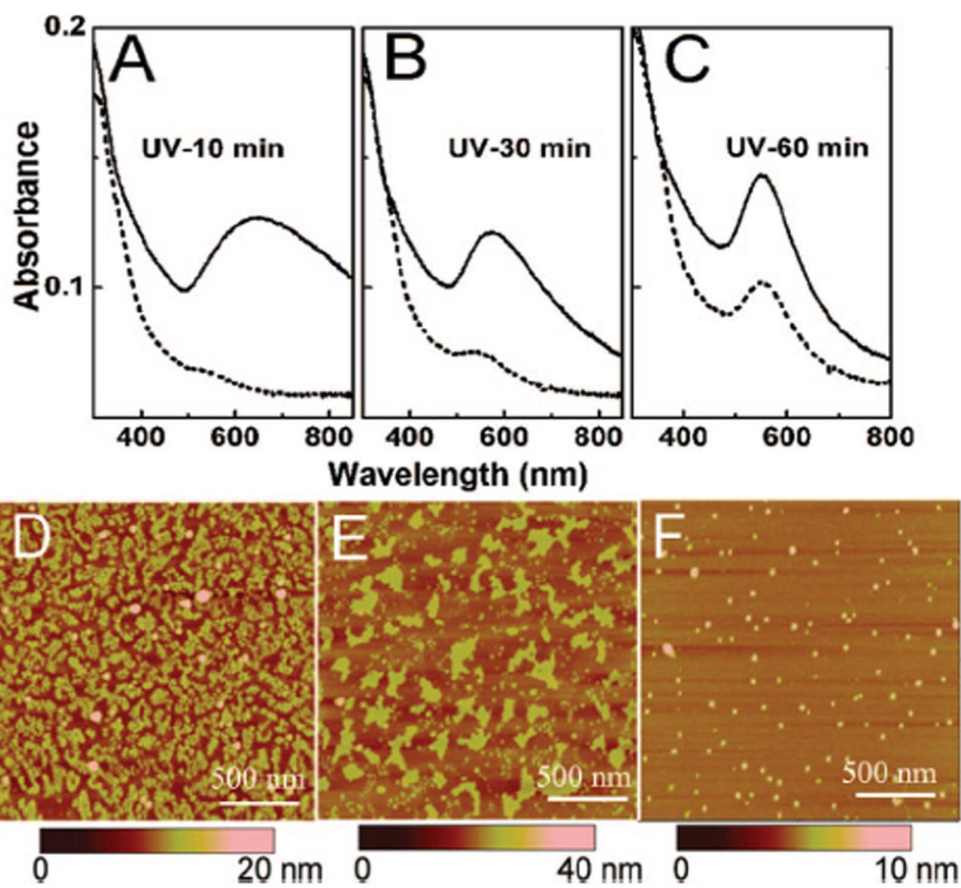

Figure 12. UV–Vis spectra and AFM images of organized LB films containing gold nanoparticles.

Firstly, the effect of gemini compounds on in situ self-assembly and fabrication of gold nanoparticles in organized molecular films have been demonstrated [42]. In comparison with traditional compounds, gemini molecules demonstrated well the capacity to fix chloroaurate ions onto various solid substrates, suggesting an important route to prepare metallic nano-particles in organized films by chemical reduction method. In addition, gemini compounds could produce a 2D confined environment in LB films to accommodate the formed gold nanoparticles. Thus, the size, shape, and interparticle distances can be regulated by changing various reducing methods. Various nanostructures could be fabricated, such as nanoparticles,

nanowires, and the tree-branched domains. Based on the obtained experimental results, different gold nanostructures could be synthesized by regulating various reductants or reducing processes. Moreover, we tried to control gold nanostructures by optical method. The obtained composite film was irradiated with UV light and then reduced by $AuCl_4^-$ ions with hydroquinone, as seen in Figure 12. The present research work provided the new clue for the synthesis of metallic particles in films from special compounds, showing important exploration in designing various gold nanostructures.

In addition, we presented a facile synthetic method to the gold nanostructures using a series of gemini amphiphiles through liquid–liquid biphase method [43]. The gemini amphiphiles themselves could serve as both capping and reducing agents. The spacer and concentration of the gemini amphiphiles played an important role in the formation of gold nanoprisms. It is predicted that gold and other novel metal nanostructures may be produced by gemini amphiphiles whose properties can be well controlled by designing different headgroups, spacers, or alkyl chains. In order to make clear the gold nanostructures, the chloroform solution was cast onto copper grid for TEM measurement, as shown in Figure 13. For gold nanostructures generated by GN1, a few polygon gold nanoparticles were found. In contrast, uniform gold nanoparticles with a size of 11.4 ± 1.2 nm were observed in GN2 chloroform solution. Interestingly, in GN3 chloroform solution, triangular nanoplates and nanoparticles were both observed. The obvious difference suggests that the spacer has an influence on the shapes of gold nanostructures. On the other hand, no gold nanoparticle can be observed in aqueous phase no matter how long the reaction proceeded.

Considering the above research background, we have prepared new kinds of gold nanoparticles via some bolaform Schiff base compounds with hydrophilic spacers and aromatic headgroups in molecular skeletons [44]. By stirring the mixed solution of aqueous $AuCl_4^-$ ions with chloroform solution of used Schiff base molecules, the metal ions shifted to the chloroform phase and reduced to the formation of different gold nanoparticles. The data indicated that different gold nanostructures could be obtained by regulating the molecular skeletons of used bolaform compounds, including spacers and headgroups, as well as the relative ratios of compounds to metal ions. In addition, the characterization of morphologies and spectra indicated that the present designed bolaform amphiphilic compounds could act as both capping agents and reducing agents. So the UV–Vis spectra in different conditions are demonstrated, as seen in Figure 14. From the obtained UV–Vis data, it clearly indicated that the spacer and azomethine segments in bolaform molecules could be positively charged at interface in transferred process. In addition, the photocatalytic capacity of the obtained gold nanoparticles on dye degradation was demonstrated in Figure 15, showing the influence of molecular skeletons in the used compounds on the regulation of prepared gold nanoparticles and next catalytic behaviors. The present obtained data suggested that various gold nanostructures could be designed and synthesized by changing substituted skeletons in used template compounds
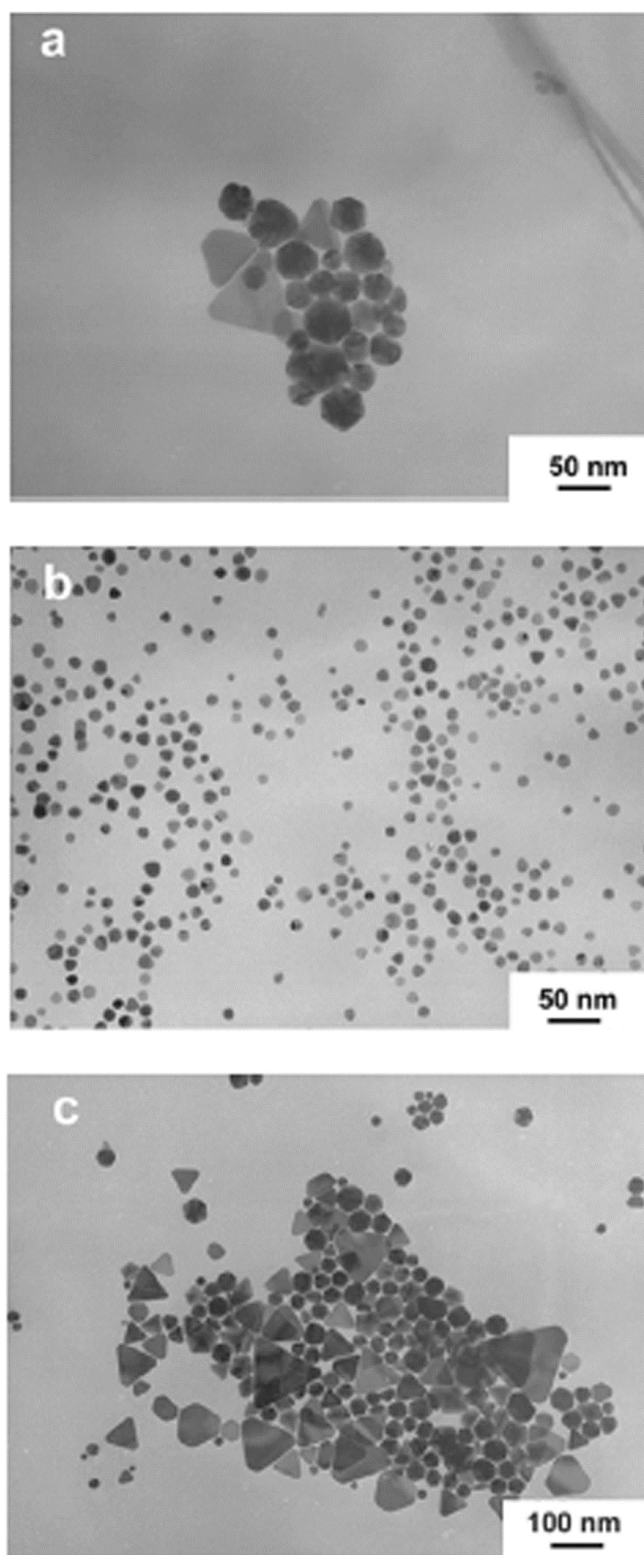
Figure 13. TEM images of reduced gold in GN1 (a), GN2 (b), and GN3 (c) chloroform solution after 36 h of reaction respectively.
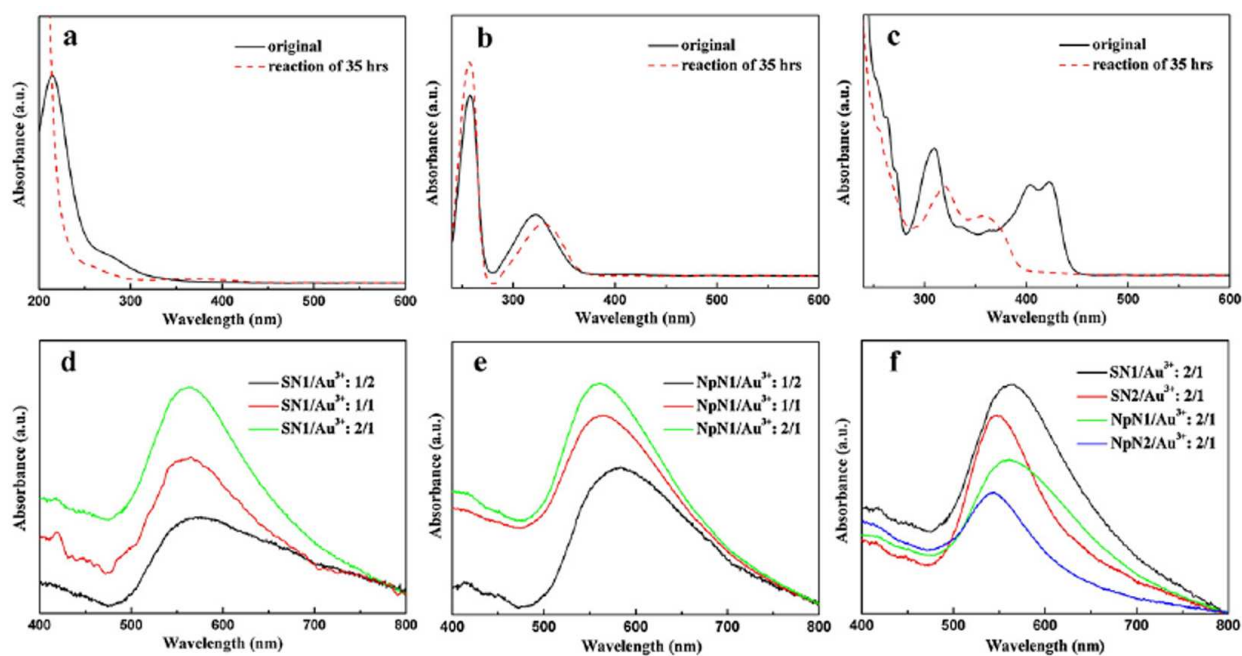
Figure 14. UV–Vis spectra of 0.1 mM AuCl$_4^-$ ions and prepared gold nanostructures in aqueous solution.
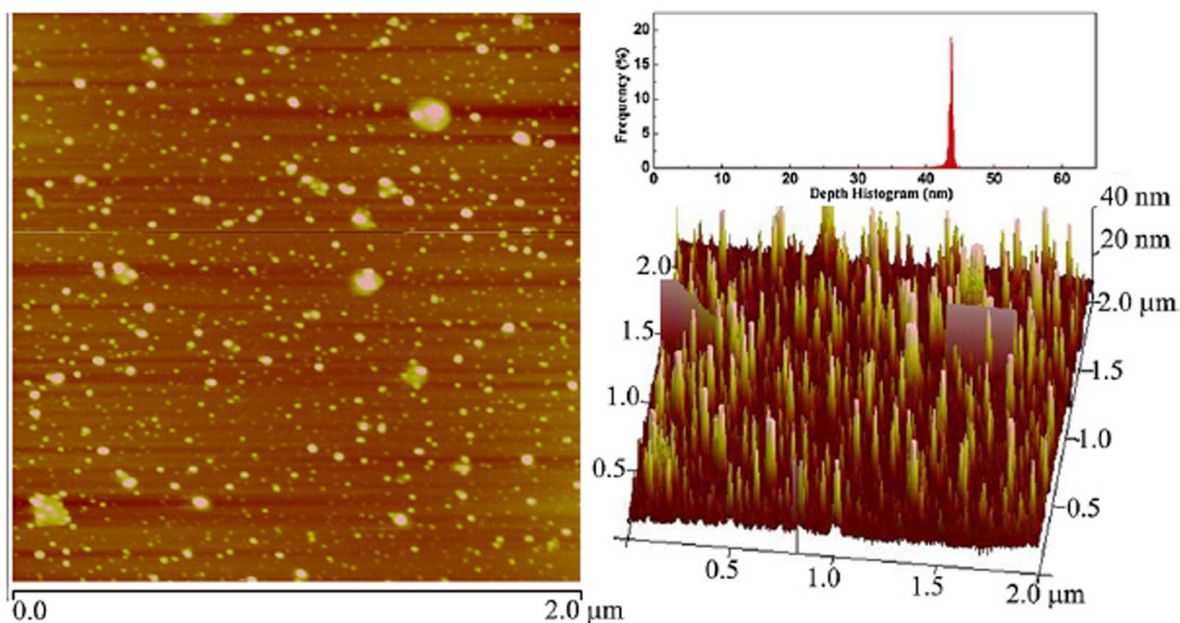

Figure 15. AFM images of height and 3D surface plot view with depth histogram of gold nanoparticles on mica prepared from instant ultrasonic ethanol solution with SN2 to chloroaurate ion ratio of 2:1 after 35 h of reaction.

In addition, some other gold nanoparticles were synthesized by two bolaform cholesteryl imide derivatives with different lengths of ethyleneamine spacers at a liquid–liquid interface [45]. Spectral and morphological measurements indicated that both bolaform amphiphiles could act as both capping agents and reducing agents. To further characterize the prepared

gold nanostructures, TEM measurements have been demonstrated, as seen Figure 16. The images indicated that the size distribution of obtained gold nanostructures could be regulated by changing various spacers in used molecular skeletons. In addition, the effect of molar ratio of the template compound to $AuCl_4^-$ ions was also investigated in details. The experimental data indicated that various nanostructures, such as hexagonal, polygon nanoparticles, and nanoplates, could be synthesized. Moreover, the photocatalytic capacity of prepared gold nanostructures on dye degradation was also characterized, suggesting the importance of compounds' skeletons in regulating the formation of gold nanoparticles and changing relative catalytic properties, as demonstrated in Figure 17. The obtained research data would give new clue for the preparation of gold nanostructures by designing special template compounds.
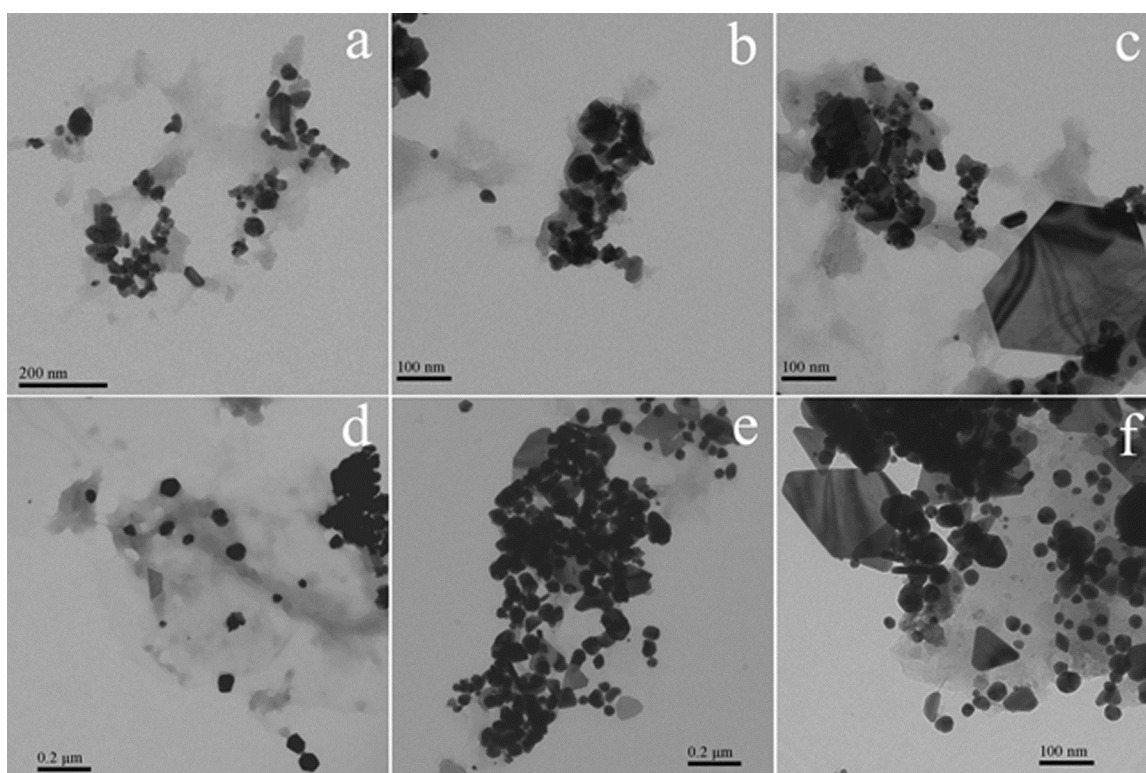

Figure 16. TEM images of gold nanoparticles by using different compounds to chloroaurate ion ratio.

4. Conclusion and perspectives

We are working on the preparation, self-assembly, and application of functionalized nano-composites and nanomaterials. In this chapter, various kinds of nanocomposites including graphene nanocomposites and gold nanoparticles have been designed and characterized. For preparation of graphene composites, hybridization with functional little organic molecules, polymers, and various metal oxides/salts have been achieved, and the self-assembly process and photocatalytic capacities have also been demonstrated. As for the synthesis of gold
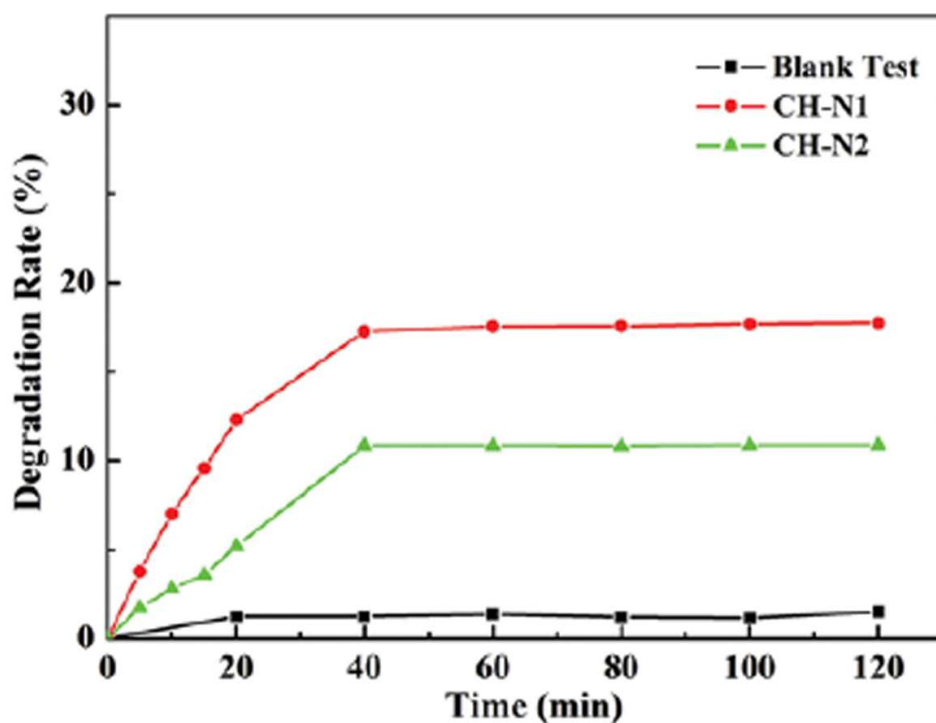
Figure 17. Photocatalytic activities of gold nanoparticles by using two amphiphiles with amphiphile to chloroaurate ion ratio of 2:1 on the degradation of methyl orange.

nanoparticles, the different prepared conditions, such as LB films/bulk, molecular skeletons/ substituted headgroups, and kinds of template compounds, have been investigated to control and regulate the designed gold nanostructures. Thus, the photocatalytic behaviors of as-obtained gold nanoparticles on dyes degradation were also characterized. The above-mentioned research work may provide new and potential perspective for the preparation and analysis of nanocomposite and nanomaterials. In closing, in recent several decades, preparation of novel nanocomposites are promising and emerging as attentive research platforms based on special properties and application fields. In addition, the self-assembly techniques belonging to supramolecular chemistry seem to be key subject in physical chemistry, related to various fundamental and scientific fields such as electron and energy transfer, organic electronics, catalysis engineering, and so on. Thus, the present preliminary research works only give a cursory browse of recent progress in this field. Future research orientation on synthesis of nanocomposites and nanomaterials would mainly focus on the special nanostructures with less-expensive fabrication process to gain high-performance and low-cost nanocomposite and nano-devices.

Acknowledgements

Author details

Jingxin Zhou[1], Tifeng Jiao[1,2*], Qingrui Zhang[1] and Jie Hu[1]

*Address all correspondence to: tfjiao@ysu.edu.cn

1 Hebei Key Laboratory of Applied Chemistry, School of Environmental and Chemical Engineering, Yanshan University, Qinhuangdao, P. R. China

2 National Key Laboratory of Biochemical Engineering, Institute of Process Engineering, Chinese Academy of Sciences, Beijing, P. R. China

References

[1]   Mutiso RM, Winey KI. Electrical properties of polymer nanocomposites containing rod-like nanofillers. *Prog Polymer Sci* 2015;40:63–84.

[2]   Campbell TA, Ivanova OS. 3D printing of multifunctional nanocomposites. *Nano Today* 2013;8(2):119–20.

[3]   Vashist SK, Luong JHT. Recent advances in electrochemical biosensing schemes using graphene and graphene-based nanocomposites. *Carbon* 2015;84:519–50.

[4]   Hu K, Kulkarni DD, Choi I, Tsukruk VV. Graphene-polymer nanocomposites for structural and functional applications. *Prog Polymer Sci* 2014;39(11):1934–72.

[5]   Jiao T, Hu J, Zhang Q, Xiao Y. Preparation and self-assembly of functionalized nanocomposites and nanomaterials-relationship between structures and properties. In: Larramendy M. (ed.) *Nanomaterials–Toxicity and Risk Assessment*. Rijeka: InTech; 2015, pp. 177–210.

[6]   Jiao T, Wang S, Zhou J. Molecular design and supramolecular assemblies of novel amphiphiles with special molecular structures in organized molecular films. In: Rahman M. (ed.) *Nanomaterials*. Rijeka: InTech; 2011, pp. 315–46.

[7] Lee YS. *Self-Assembly and Nanotechnology Systems: Design, Characterization, and Applications*. New Jersey: John Wiley & Sons, Inc.; 2011, pp. 111–40.

[8] Jiao T, Wang Y, Zhang Q, Zhou J, Gao F. Regulation of substituent groups on morphologies and self-assembly of organogels based on some azobenzene imide derivatives. *Nanoscale Res Lett* 2013;8:160.

[9] Jiao T, Huang Q, Zhang Q, Xiao D, Zhou J, Gao F. Self-assembly of organogels via new luminol imide derivatives: diverse nanostructures and substituent chain effect. *Nanoscale Res Lett* 2013;8:278.

[10] Jiao T, Gao F, Zhang Q, Zhou J, Gao F. Spacer effect on nanostructures and self-assembly in organogels via some bolaform cholesteryl imide derivatives with different spacers. *Nanoscale Res Lett* 2013;8:406.

[11] Liang D, Cui C, Hu H, Wang Y, Xu S, Ying B, Li P, Lu B, Shen H. One-step hydrothermal synthesis of anatase TiO_2/reduced graphene oxide nanocomposites with enhanced photocatalytic activity. *J Alloys Compd* 2014;582:236–40.

[12] Ullah K, Zhu L, Meng ZD, Ye S, Sun Q, Oh WC. A facile and fast synthesis of novel composite Pt-graphene/TiO_2 with enhanced photocatalytic activity under UV/Visible light. *Chem Eng J* 2013;231:76–83.

[13] Bai XJ, Wang L, Zhu YF. Visible photocatalytic activity enhancement of $ZnWO_4$ by graphene hybridization. *ACS Catal* 2012;2:2769–78.

[14] Sun L, Shao R, Tang LQ, Chen ZD. Synthesis of $ZnFe_2O_4$/ZnO nanocomposites immobilized on graphene with enhanced photocatalytic activity under solar light irradiation. *J Alloys Compd* 2013;564:55–62.

[15] Xu JJ, Ao YH, Chen MD. A simple method for the preparation of Bi_2WO_6-reduced graphene oxide with enhanced photocatalytic activity under visible light irradiation. *Mater Lett* 2013;92:126–8.

[16] Li T, Shen JF, Li N, Ye MX. Hydrothermal preparation, characterization and enhanced properties of reduced graphene-$BiFeO_3$ nanocomposite. *Mater Lett* 2013;91:42–4.

[17] Lv T, Pan LK, Liu XJ, Lu T, Zhu G, Sun Z. Enhanced photocatalytic degradation of methylene blue by ZnO-reduced graphene oxide composite synthesized via microwave-assisted reaction. *J Alloys Compd* 2011;509:10086–91.

[18] Jiang LX, Li KX, Yan LS, Dai YH, Huang ZM. Preparation of Ag(Au)/graphene-TiO_2 composite photocatalysts and their catalytic performance under simulated sunlight irradiation. *Chin J Catal* 2012;33(12):1974–81.

[19] Zhang DF, Pu XP, Ding GQ, Shao X, Gao YY, Liu JX, Gao MC, Li Y. Two-phase hydrothermal synthesis of TiO_2-graphene hybrids with improved photocatalytic activity. *J Alloys Compd* 2013;572:199–204.

[20] Ghosh SK, Pal T. Interparticle coupling effect on the surface plasmon resonance of gold nanoparticles: from theory to applications. *Chem Rev* 2007;107:4797–862.

[21] Katz E, Willner I. Integrated nanoparticle-biomolecule hybrid systems: synthesis, properties, and applications. *Angewandte Chemie International Edition* 2004;43(45): 6042–108.

[22] Daniel MC, Astruc D. Gold nanoparticles: assembly, supramolecular chemistry, quantum-size-related properties, and applications toward biology, catalysis, and nanotechnology. *Chem Rev* 2004;104:293–346.

[23] Liao J, Bernard L, Langer M, Schoenberger C, Calame M. Reversible formation of molecular junctions in 2D nanoparticle arrays. *Adv Mater* 2006;18(18):2444–7.

[24] Klajn R, Bishop KJM, Grzybowski BA. Light-controlled self-assembly of reversible and irreversible nanoparticle suprastructures. *Proc Nat Acad Sci USA* 2007;104:10305–9.

[25] Koplin E, Niemeyer CM, Simon U. Formation of electrically conducting DNA-assembled gold nanoparticle monolayers. *J Mater Chem* 2006;16:1338–44.

[26] Meister A, Drescher S, Mey I, Wahab M, Graf G, Garamus VM, Hause G, Mo1gel HJ, Janshoff A, Dobner B, Blume A. Helical nanofibers of self-assembled bipolar phospholipids as template for gold nanoparticles. *J Phys Chem B* 2008;112:4506–11.

[27] Jadzinsky PD, Calero G, Ackerson CJ, Bushnell DA, Kornberg RD. Structure of a thiol monolayer-protected gold nanoparticle at 1.1 Å resolution. *Science* 2007;318:430–3.

[28] Wen Y, Jiang X, Yin G, Yin J. Multi-responsive amphiphilic gold nanoparticles (AuNPs) protected by poly(ether amine) (PEA). *Chem Commun* 2009;43:6595–7.

[29] Song WJ, Du JZ, Sun TM, Zhang PZ, Wang J. Gold nanoparticles capped with polyethyleneimine for enhanced siRNA delivery. *Small* 2010;6:239–46.

[30] Ko S, Park TJ, Kim HS, Kim JH, Cho YJ. Directed self-assembly of gold binding polypeptide-protein: a fusion proteins for development of gold nanoparticle-based SPR immunosensors. *Biosens Bioelectron* 2009;24:2592–7.

[31] George J, Thomas KG. Surface plasmon coupled circular dichroism of Au nanoparticles on peptide nanotubes. *J Am Chem Soc* 2010;132:2502–3.

[32] Cho EC, Au L, Zhang Q, Xia Y. The effects of size, shape, and surface functional group of gold nanostructures on their adsorption and internalization by cells. *Small* 2010;6:517–22.

[33] Jiao T, Wang Y, Zhang Q, Yan X, Zhao X, Zhou J, Gao F. Self-assembly and headgroup effect in nanostructured organogels via cationic amphiphile-graphene oxide composites. *PLoS ONE* 2014;9(7):e101620.

[34] Jiao T, Wang Y, Zhang Q, Yan X, Zhao X, Huo Q, Zhou J, Gao F. Organogels via gemini amphiphile-graphene oxide composites: self-assembly and symmetry effect. *Sci Adv Mater* 2015;7(9):1677–85.

[35] Jiao T, Guo H, Zhang Q, Peng Q, Tang Y, Yan X, Li B. Reduced graphene oxide-based silver nanoparticle-containing composite hydrogel as highly efficient dye catalysts for wastewater treatment. *Sci Rep-UK* 2015;5:11873.

[36] Hu J, Ma J, Wang L, Huang H. Synthesis and photocatalytic properties of LaMnO$_3$-graphene nanocomposites. *J Alloys Compd* 2014;583:539–45.

[37] Hu J, Ma J, Wang L, Huang H. Preparation of La$_{1-x}$Sr$_x$MnO$_3$ /graphene thin films and their photocatalytic activity. *Mater Sci Eng B* 2014;180:46–53.

[38] Hu J, Ma J, Wang L, Huang H, Ma L. Preparation, characterization and photocatalytic activity of Co-doped LaMnO$_3$/graphene composites, *Powder Technol* 2014;254:556–62.

[39] Hu J, Wang L, Ma J, Huang H. Study on the preparation and photocatalytic performance of the LaNiO$_3$/graphene composite film. *Rare Metal Mater Eng* 2014;43(7):1736–41.

[40] Hu J, Wang L, Shi L, Huang H. Preparation of La$_{1-x}$Ca$_x$MnO$_3$ perovskite-graphene composites as oxygen reduction reaction electrocatalyst in alkaline medium. *J Power Sources* 2014;269:144–51.

[41] Hu J, Men J, Ma J, Huang H. Preparation of LaMnO$_3$/graphene thin films and their photocatalytic activity. *J Rare Earths* 2014;32(12):1127–35.

[42] Zhong L, Jiao T, Liu M. Synthesis and assembly of gold nanoparticles in organized molecular films of gemini amphiphiles. *Langmuir* 2008;24:11677–83.

[43] Zhong L, Jiao T, Liu M. A facile method to the synthesis of gold nanoprisms using a series of gemini amphiphiles. *J Nanosci Nanotechnol* 2009;9:2726–30.

[44] Jiao T, Wang Y, Guo W, Zhang Q, Yan X, Chen J, Wang L, Xie D, Gao F. Synthesis and photocatalytic property of gold nanoparticles by using a series of bolaform Schiff base amphiphiles. *Mater Res Bull* 2012;47(12):4203–9.

[45] Jiao T, Wang Y, Zhang Q, Yan X, Chen J, Zhou J, Gao F. Preparation and photocatalytic property of gold nanoparticles by using two bolaform cholesteryl imide derivatives. *J Dispers Sci Technol* 2013;34(12):1675–82.